3098 *Organometallics* **2010,** *29,* 3098–3108
DOI: 10.1021/om100153z

ORGANOMETALLICS
Article

Synthesis and Catalytic Reactivity of Bis(alkylzinc)-hydride-di(2-pyridylmethyl)amides

Marcel Kahnes,[†] Helmar Görls,[†] Leticia González,[‡] and Matthias Westerhausen*,[†]

[†]*Institut für Anorganische und Analytische Chemie, Friedrich-Schiller-Universität Jena, August-Bebel-Strasse 2, 07743 Jena, Germany, and* [‡]*Institut für Physikalische Chemie, Friedrich-Schiller-Universität Jena, Helmholtzweg 4, 07743 Jena, Germany*

Received February 25, 2010

Direct zincation of dipicolylamin (DPA) and alcohols (MeOH, *i*PrOH, *t*BuOH) with dialkylzinc gives bis(alkylzinc)alkoxide-di(2-pyridylmethyl)amides {alkyl = methyl (**1**, **2**), trimethylsilylmethyl (**3**), bis-(trimethylsilyl)methyl (**4**), alkoxide = OMe, O*i*Pr, O*t*Bu} possessing a central four-membered Zn_2NO unit. Treatment of these alkoxides **1**−**4** with arylsilanes leads to an exchange of the (μ-OR′) moiety, yielding the corresponding hydrides $[(RZn)_2(\mu\text{-H})\{\mu\text{-N}(CH_2Py)_2\}]$ {R = Me (**6**), CH_2SiMe_3 (**7**), $CH(SiMe_3)_2$ (**8**)}. Hydride **6** reacts with tBuNH$_2$ to form the corresponding amide $[(MeZn)_2\{\mu\text{-N(H)}t\text{Bu}\}\{\mu\text{-N}(CH_2Py)_2\}]$ (**5**) and adds acetone to yield **2** again. The trimethylsilyl-substituted derivative **7** undergoes spontaneous conversion to form the pentanuclear zinc hydride-bridged dimer $[\{Me_3SiCH_2Zn\}_4\{Zn(\mu\text{-H})_4\}\{\mu\text{-N}(CH_2Py)_2\}_2]$ (**9**). The new hydride complexes were characterized in solution and in the solid state including single-crystal X-ray analysis of **8** and **9**. Both hydrides **6**−**8** and alkoxides **1**−**4** were found to catalyze the hydrosilylation of aldehydes and ketones effectively. The variation of the zinc-bound alkyl group facilitates control over the catalyst reactivity by steric and electronic means. In order to achieve a deeper insight into the mechanism and the role of the cocatalytic Zn(II) centers, extensive DFT calculations were performed. In the two-step catalytic process the ketone first coordinates to one catalytic center of **6** and thus cleaves a Zn−(μ-H) bond. A subsequent intramolecular hydride transfer leads to the formation of the bridged dinuclear zinc alkoxide being the most stable species in this cycle. In the second half of the cycle, possessing the highest activation barrier, the silane inserts into a Zn−O bond, forming a six-membered ring with a Zn[μ-(H−Si−O)]Zn moiety. Consecutive cleavage of the Si−H_{Zn} and Zn−O bonds regenerates the zinc hydride **6** along with the formation of the silyl ether. NMR spectroscopic studies support these findings.

Introduction

In the early 1950s zinc hydride (ZnH_2) was described as a white solid with low volatility and solubility, presumably a highly associated, hydrogen-bridged coordination polymer.[1] However, ZnH_2 readily dissolves in pyridine under formation of a new complex reported as $C_5H_6NZn_3H_5\cdot 2$py. A prolonged reaction period gives bis(l,4-dihydro-1-pyridyl)zinc, which shows some interesting reducing properties toward carbonyls.[2] In the presence of diorganylzinc compounds and two equivalents of pyridine, ZnH_2 dismutates to form RZnH·py (R = Et, Ph), which is trimeric in solution. However, these solutions decompose within a few hours at room temperature, as indicated by the precipitation of zinc metal.[3]

Besides aromatic nitrogen donors the aliphatic trimethylethylenediamine also reacts with zinc hydride, yielding 2-dimethylaminoethyl(methyl)amidozinc hydride (**A**) (see Scheme 1). This dimeric complex is the first structurally characterized zinc hydride with a terminally bound hydride exhibiting a Zn−H bond length of 161.8(6) pm.[4] Stabilization and isolation of terminal hydrides also succeeds with the application of sterically demanding ligands such as the tris(3-*tert*-butylpyrazolyl)hydroborate [Tp^{Bu^t}] or aryl-substituted β-diketiminate anions [HC(CMeNAr*)$_2$]$^-$. The reaction of ZnH_2 with Tl[Tp^{Bu^t}] gives the desired monomeric complex **B**, being also accessible by the conversion of the fluoride [$Tp^{p\text{-Tol,Me}}$]ZnF with Et_3SiH.[5] Depending on the steric demands of the N-bound aryl group (Ar*), the β-diketiminate zinc hydride complexes crystallize either monomeric (Ar* = 2,6-iPr$_2$C$_6$H$_3$) with a terminal hydride (Zn−H 146(2) pm) in **C**[6] or dimeric with bridging hydrides as in complex **D**. The latter was synthesized in a metathesis reaction of

*To whom correspondence should be addressed. E-mail: m.we@uni-jena.de.

(1) (a) Finholt, A. E.; A. C. Bond, J.; Schlesinger, H. I. *J. Am. Chem. Soc.* **1947**, *69*, 1199–1203. (b) Barbaras, G. D.; Dillard, C.; Finholt, A. E.; Wartik, T.; Wilzbach, K. E.; Schlesinger, H. I. *J. Am. Chem. Soc.* **1951**, *73*, 4585–4590. For a review see: (c) Aldridge, S.; Downs, A. *J. Chem. Rev.* **2001**, *101*, 3305–3366.

(2) (a) de Koning, A. J.; Boersma, J.; van der Kerk, G. J. M. *Tetrahedron Lett.* **1977**, *18*, 2547–2548. (b) de Koning, A. J.; Boersma, J.; van der Kerk, G. J. M. *J. Organomet. Chem.* **1980**, *186*, 159–172. (c) de Koning, A. J.; Boersma, J.; van der Kerk, G. J. M. *J. Organomet. Chem.* **1980**, *186*, 173–184.

(3) (a) de Koning, A.; Boersma, J.; van der Kerk, G. *J. Organomet. Chem.* **1978**, *155*, C5–C7. (b) Koning, A. J. D.; Boersma, J.; Van Der Kerk, G. J. M. *J. Organomet. Chem.* **1980**, *195*, 1–12.

(4) (a) Bell, N. A.; Coates, G. E. J. *Chem. Soc. A* **1968**, 823–826. (b) Bell, N. A.; Moseley, P. T.; Shearer, H. M. M.; Spencer, C. B. *Acta Crystallogr.* **1980**, *B36*, 2950–2954.

(5) (a) Han, R.; Gorrell, I. B.; Looney, A. G.; Parkin, G. *Chem. Commun.* **1991**, 717–719. (b) Looney, A.; Han, R.; Gorrell, I. B.; Cornebise, M.; Yoon, K.; Parkin, G.; Rheingold, A. L. *Organometallics* **1995**, *114*, 274–288. (c) Kläui, W.; Schilde, U.; Schmidt, M. *Inorg. Chem.* **1997**, *36*, 1598–1601.

(6) Spielmann, J.; Piesik, D.; Wittkamp, B.; Jansen, G.; Harder, S. *Chem. Commun.* **2009**, 3455–3456.

 Published on Web 06/28/2010 © 2010 American Chemical Society

Scheme 1. Isolated Zinc Hydrides with Additional Nitrogen, Oxygen, and Carbon Donors

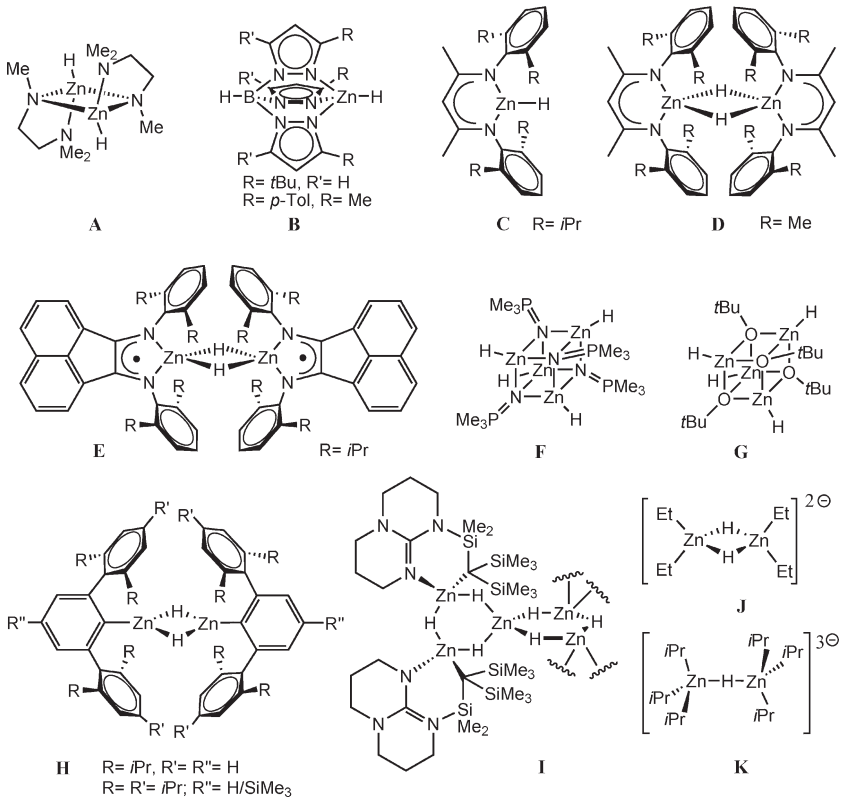

the corresponding fluoride with triethylsilane.[7] The diimine radical anions in **E** also support the four-membered Zn_2H_2 unit with bridging hydrides.[8] Heterocubane structures with a Zn_4N_4 cubic skeleton in **F**[9] or a cluster core consisting of a $[(HZnOtBu)_{4-n}(LiOtBu)_n]$ ($n = 0-3$) framework as in **G**[10] are able to stabilize hydrido ligands in terminal exocyclic positions. The advantageous oligonuclear nature of the hydridozinc alkoxide cubane clusters facilitates hydrogenation of CO_2 proceeding most rapidly with the heteronuclear monolithium cluster.[11]

Besides nitrogen and oxygen donors sterically demanding alkyl and phenyl groups are suitable ligands in order to stabilize zinc hydride species. Treatment of dimeric arylzinc iodide Ar′Zn(μ-I)$_2$ZnAr′ with NaH leads to the hydride-bridged dimer Ar′Zn(μ-H)$_2$ZnAr′ **H**. Furthermore the iodide Ar′Zn(μ-I)$_2$ZnAr′ can be reduced with sodium metal, yielding Ar′ZnZnAr′ with a Zn−Zn bond.[12] Similarly the dimeric alkylzinc bromide RZn(μ-Br)$_2$ZnR (R being a bulky trissilylmethyl with the bicyclic 1,3,4,6,7,8-hexahydro-2*H*-pyrimido[1,2-*a*]pyrimidine unit) reacts with an excess of NaH, yielding the oligomeric hydride-bridged complex **I**.[13] When neat dialkylzinc (alkyl = Et, *i*Pr) is mildly heated together with sodium, the corresponding zincates **J** and **K** are formed. Crystal structure analysis revealed the presence of bridging hydrides originating from a β-hydride elimination.[14] The existence of alkali metal hydrido dialkylzincate species $MHZnR_2$ (M = Li, Na), prepared from dialkylzinc and excess alkali metal hydride in ethereal solutions, has already been proposed by Shriver and co-workers.[15] These hydridozincate complexes have shown to effectively reduce esters and amides as well as aldehydes and ketones with a reactivity comparable to $LiAlH_4$.[16,17] Moreover the dialkyzinc alkali metal hydride system can be applied to a catalytic hydride transfer.[17] In addition to metal hydrides silanes can also serve as hydride source. The zinc-promoted hydrosilylation therefore has been the subject of great interest for the past decade.[18−24] Especially the advantageous properties of polymethylhydrosiloxane (PMHS), which is an

(7) Hao, H.; Cui, C.; Roesky, H. W.; Bai, G.; Schmidt, H.-G.; Noltemeyer, M. *Chem. Commun.* **2001**, 1118–1119.
(8) Fedushkin, I. L.; Eremenko, O. V.; Skatova, A. A.; Piskunov, A. V.; Fukin, G. K.; Ketkov, S. Y.; Irran, E.; Schumann, H. *Organometallics* **2009**, *28*, 3863–3868.
(9) (a) Krieger, M.; Neumüller, B.; Dehnicke, K. *Z. Anorg. Allg. Chem.* **1998**, *624*, 1563–1564. (b) Krieger, M.; Gould, R. O.; Neumüller, B.; Harms, K.; Dehnicke, K. *Z. Anorg. Allg. Chem.* **1998**, *624*, 1434–1442.
(10) Marciniak, W.; Merz, K.; Moreno, M.; Driess, M. *Organometallics* **2006**, *25*, 4931–4933.
(11) Merz, K.; Moreno, M.; Löffler, E.; Khodeir, L.; Rittermeier, A.; Fink, K.; Kotsis, K.; Muhler, M.; Driess, M. *Chem. Commun.* **2008**, 73–75.
(12) (a) Zhu, Z.; Wright, R. J.; Olmstead, M. M.; Rivard, E.; Brynda, M.; Power, P. P. *Angew. Chem.* **2006**, *118*, 5939–5942. (b) Zhu, Z.; Wright, R. J.; Olmstead, M. M.; Rivard, E.; Brynda, M.; Power, P. P. *Angew. Chem., Int. Ed.* **2006**, *45*, 5807–5810. (c) Zhu, Z.; Brynda, M.; Wright, R. J.; Fischer, R. C.; Merrill, W. A.; Rivard, E.; Wolf, R.; Fettinger, J. C.; Olmstead, M. M.; Power, P. P. *J. Am. Chem. Soc.* **2007**, *129*, 10847–10857. (d) Zhu, Z.; Fettinger, J. C.; Olmstead, M. M.; Power, P. P. *Organometallics* **2009**, *28*, 2091–2095.
(13) Coles, M. P.; El-Hamruni, S. M.; Smith, J. D.; Hitchcock, P. B. *Angew. Chem., Int. Ed.* **2008**, *47*, 10147–10150.
(14) Lennartson, A.; Hakansson, M.; Jagner, S. *Angew. Chem., Int. Ed.* **2007**, *46*, 6678–6680.
(15) Kubas, G. J.; Shriver, D. F. *J. Am. Chem. Soc.* **1970**, *92*, 1949–1954.
(16) Shriver, D. F.; Kubas, G. J.; Marshall, J. A. *J. Am. Chem. Soc.* **1971**, *93*, 5076–5079.
(17) Uchiyama, M.; Furumoto, S.; Saito, M.; Kondo, Y.; Sakamoto, T. *J. Am. Chem. Soc.* **1997**, *119*, 11425–11433.
(18) (a) Mimoun, H.; de Saint Laumer, J. Y.; Giannini, L.; Scopelliti, R.; Floriani, C. *J. Am. Chem. Soc.* **1999**, *121*, 6158–6166. (b) Mimoun, H. *J. Org. Chem.* **1999**, *64*, 2582–2589.
(19) (a) Bette, V.; Mortreux, A.; Lehmann, C. W.; Carpentier, J.-F. *Chem. Commun.* **2003**, 332–333. (b) Bette, V.; Mortreux, A.; Savoia, D.; Carpentier, J.-F. *Tetrahedron* **2004**, *60*, 2837–2842. (c) Bette, V.; Mortreux, A.; Savoia, D.; Carpentier, J.-F. *Adv. Synth. Catal.* **2005**, *347*, 289–302.
(20) Mastranzo, V. M.; Quintero, L.; de Parrodi, C. A.; Juaristi, E.; Walsh, P. J. *Tetrahedron* **2004**, *60*, 1781–1789.
(21) Gérard, S.; Pressel, Y.; Riant, O. *Tetrahedron: Asymmetry* **2005**, *16*, 1889–1891.
(22) Ushio, H.; Mikami, K. *Tetrahedron Lett.* **2005**, *46*, 2903–2906.
(23) Bandini, M.; Melucci, M.; Piccinelli, F.; Sinisi, R.; Tommasi, S.; Umani-Ronchi, A. *Chem. Commun.* **2007**, 4519–4521.

Scheme 2. Synthesis of Precatalyst Species for the Zinc-Catalyzed Hydrosilylation

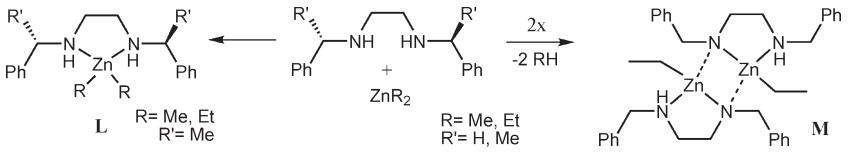

air-stable, inexpensive, and nontoxic hydride source, has opened new perspectives for this method. The catalyst system, usually being composed of a cheap, readily available zinc precursor ($ZnEt_2$, $Zn(OMe)_2$, $Zn(OH)_2$ $Zn(OOCR)_2$) and a 1,2-diamine or diimine, is able to reduce a variety of subtrates such as aldehydes, ketones, imines, esters, lactones, and epoxides.[18−20,22] These reductions proceed under mild conditions with catalyst loads of 2−5 mol %. In the asymmetric hydrosilylation, requiring chiral diamines, *N*,*N*′-ethylenebis(1-arylethylamine) ligands achieve an enantiomeric excess up to 96%[22] depending on the nature of the aryl substituent. N,S-Chelating ligands turned out to be less enantioselective.[21,23] Working with an excess of silane even allows carrying out the reaction in protic solvents such as MeOH.[19]

Although extensively exploited, the true nature of the in situ formed catalyst still remains unclear. Dialkylzinc (alkyl = Me, Et) forms a stable adduct **L** with *N*,*N*′-ethylenebis(1-phenylethylamine) and metalates *N*,*N*′-ethylenebis(benzylamine) to give the dimeric amide **M** (see Scheme 2).[18,19] When operating in aprotic solvents, the precurser complexes **L** and **M** are believed to convert into a monomeric nitrogen donor-stabilized alkyl zinc hydride species.

Recently, Issenhuth et al. developed a detailed mechanism based on density functional theoretical calculations for the enantioselective hydrosilylation of ketones catalyzed by isoelectronic Cu(I) diphosphane complexes. According to the calculations the two-step catalytic cycle involves copper alkoxides and hydrides, comparable to the suggested zinc intermediates.[25] In any case a homonuclear single-site species with terminal hydrides rather than the dimeric forms are considered to be the active species in the catalytic cycle of d^{10} metal-promoted hydrosilylation reactions. We herein present mixed ligand zinc hydrides incorporating the stabilizing properties of both N-(amide/coordinative) and carbon donors. This new complex matches the above-described characteristics of active species in zinc-promoted hydrosilylation. Thus the complex is successfully applied in the hydrosilylation of carbonyls. Due to the lack of detailed mechanistic information, we furthermore employed extensive density functional theoretical calculations in order to shed light on the nature of the involved intermediates and transition structures. Special interest was addressed to the dinuclear nature of the zinc catalyst.

Results and Discussion

Synthesis and Structural Characterization. Synthesis of Bis(alkylzinc)-alkoxide-di(2-pyridylmethyl)amides. As reported previously[26] bis(alkylzinc)-alkoxide-di(2-pyridylmethyl)amides (**1**−**4**) are accessible by direct metalation of stoichiometric amounts of the corresponding alcohol and dipicolylamine

Scheme 3. Synthesis of Bis(alkylzinc)-alkoxide-di(2-pyridylmethyl)amides (1−4)

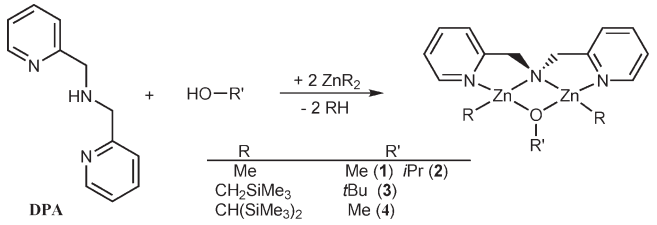

(DPA) with dialkylzinc at low temperatures (see Scheme 3). Alkylzinc alkoxides have recently gained interest as excellent precursors for the preparation of ceramic materials, nanoparticles, and ZnO films (MOCVD) with semiconducting properties.[27]

The complexes **2** and **3** as well as **4**[26] readily crystallized with the zinc atoms in distorted tetrahedral environments (see Figure 1). The endocyclic Zn1/2−N2 bond lengths in the central nearly planar Zn_2NO ring are very similar in **2**−**4** (see Table 1). Compared to the exocyclic Zn−N_{py} distances, they are shorter by 6−9 pm due to an additional electrostatic attraction. The bulkiness of the oxygen-bound alkyl group has hardly any effect on the Zn−O bond lengths. Nevertheless, the geometries of O1 are different. In **2** and **3** nearly planar environments (angle sum: 354.6° in **2** and 356.1° in **3**) are observed, whereas in **4** O1 shows a pyramidal coordination sphere (angle sum 340.5°) in order to reduce steric strain induced by the bulky bis(trimethylsilyl)methyl groups. The increasing steric demand of the organometallic alkyl substituent seems to compress the central Zn_2NO ring, resulting in slightly shorter transannular nonbonding Zn1···Zn2 distances from **2** to **4**. In addition the Zn−C bonds are elongated in this row as a consequence of steric and electronic properties of the metal-bound substituent with an increasing degree of trimethylsilyl substitution. Similar effects were observed earlier for homoleptic $Zn[CH_n(SiMe_3)_{3-n}]$.[28]

Reactivity Studies of Bis(alkylzinc)-alkoxide-di(2-pyridylmethyl)amides. The reaction of the dinuclear complexes **1** to **4** and the amide **5**[26] with phenyl- or diphenylsilane led to a complete conversion (see Scheme 4), whereas the bulkier triethylsilane did not react with these complexes. A new singlet resonance in the ^{1}H NMR spectrum in the range 3.5−5.5 ppm (C_6D_6) is indicative for a Zn−H group.[15,29] The NMR spectra of a solution of **6** also indicated the presence of minor amounts (< 5%) of a second species. Storage of the reaction solution at −20 °C for several days led to a significant

(24) Gajewy, J.; Kwit, M.; Gawronacuteski, J. *Tetrahedron: Asymmetry* **2009**, *351*, 1055–1063.
(25) Issenhuth, J.-T.; Notter, F.-P.; Dagorne, S.; Dedieu, A.; Bellemin-Laponnaz, S. *Eur. J. Inorg. Chem.* **2010**, 529–541.
(26) Kahnes, M.; Richthof, J.; Escudero, D.; Gonzaléz, L.; Westerhausen, M. *J. Organomet. Chem.* **2010**, *695*, 280–290.
(27) (a) Chandler, C. D.; Roger, C.; Hampden-Smith, M. *J. Chem. Rev.* **1993**, *93*, 1205–1241. (b) Boyle, T. J.; Bunge, S. D.; Andrews, N. L.; Matzen, L. E.; Sieg, K.; Rodriguez, M. A.; Headley, T. J. *Chem. Mater.* **2004**, *16*, 3279–3288. (c) Suh, S.; Mîinea, L. A.; Javed, S.; Hoffman, D. M. *Polyhedron* **2008**, *27*, 513–516.
(28) Westerhausen, M.; Rademacher, B.; Poll, W. *J. Organomet. Chem.* **1991**, *421* (2−3), 175–88.
(29) (a) Goeden, G. V.; Caulton, K. G. *J. Am. Chem. Soc.* **1981**, *103*, 7354–7355. (b) Neils, T. L.; Burlitch, J. M. *Inorg. Chem.* **1989**, *28*, 1607–1609.

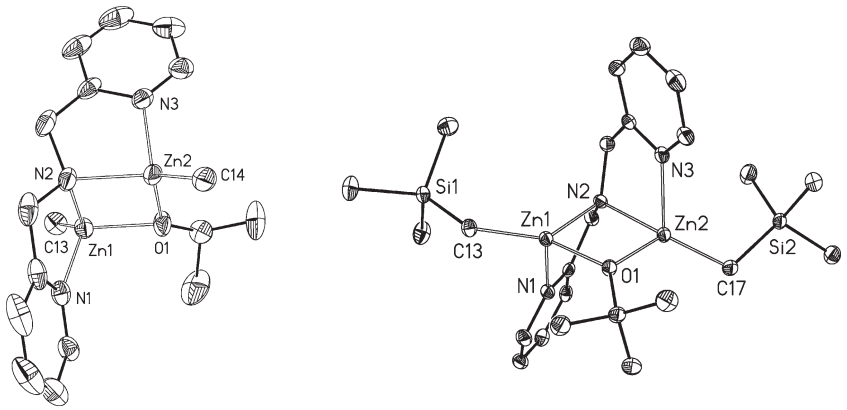

Figure 1. Molecular structures and numbering schemes of **2** (to the left) and **3** (to the right). The hydrogen atoms are omitted for clarity reasons. The ellipsoids represent a probability of 40%. Selected structural data are listed in Table 1.

Table 1. Selected Bond Lengths (pm) and Angles (deg) of 2−4 and 8

	2	3	4	8
Zn1−N1	213.4(2)	214.0(2)	215.1(3)	215.3(2)
Zn1−N2	205.3(2)	207.1(2)	205.8(3)	206.8(2)
Zn1−O1/H1	199.6(2)	198.5(2)	200.4(2)	174(3)
Zn1−C_{Zn}	197.1(3)	198.8(3)	200.3(3)	200.3(3)
Zn2−N2	205.2(2)	208.1(2)	206.7(3)	205.9(2)
Zn2−N3	213.0(2)	215.1(2)	211.9(3)	212.9(2)
Zn2−O1/H1	200.4(2)	198.0(2)	199.9(2)	182(3)
Zn2−C_{Zn}	197.1(3)	198.0(3)	200.7(3)	200.7(3)
Zn1···Zn2	293.5(1)	292.1(1)	290.4(1)	262.1(1)
Zn1−N2−Zn2	91.3(1)	89.4(1)	89.5(1)	78.9(1)
Zn1−O1/H1−Zn2	94.4(1)	94.9(1)	93.0(1)	95.0(9)
N2−Zn1−O1/H1	87.2(1)	87.9(1)	88.7(1)	94.2(9)
N2−Zn2−O1/H1	87.0(1)	87.7(1)	88.6(1)	92.0(9)
N1−Zn1−C_{Zn}	123.0(1)	110.9(1)	124.4(1)	129.2(1)
N3−Zn2−C_{Zn}	121.4(1)	122.9(1)	125.4(1)	127.6(1)
Zn1−O1−C_O	124.2(3)	133.7(1)	121.0(2)	
Zn2−O1−C_O	136.0(3)	127.5(1)	126.5(2)	

increase of the amount of degradation product along with a color change to deep orange and the precipitation of zinc metal. Similar observations were made for solutions of the pyridine complexes of the organozinc hydrides, which liberate zinc metal within a few hours at room temperature.[3]

Attempts to crystallize **6** only led to the precipitation of pale orange crystals. X-ray structure analysis revealed the formation of well-known tris(methylzinc) di(2-pyridylmethyl)amide 1,3-di(2-pyridyl)-2-azapropane-1,2-diide (**10**) as a result of an intermolecular zincation of a methylene group. Subsequent loss of a methylzinc hydride, which decomposes, could explain the zinc precipitate (Scheme 5). Complex **10** was also accessible from the reaction of dipicolylamine with dimethylzinc in a 2:3 ratio.[30] Further reactivity studies with a freshly prepared solution of **6** were performed with *tert*-butylamine and acetone in order to verify the suggested structure of **6** (see Scheme 5). Addition of one equivalent of *tert*-butylamine resulted in a vigorous evolution of hydrogen gas along with the formation of the amide **5**. Stoichiometric amounts of acetone rapidly reacted in a noticeable exothermic reaction, yielding **2** almost quantitatively.

The zinc-bound alkyl group R strongly influences the composition of the hydride species (**6**−**8**). For R = Me a bridging hydride was observed, whereas with R = CH_2SiMe_3 the nuclearity of the final product was higher. After an induction period of

(30) Westerhausen, M.; Kneifel, A. N.; Lindner, I.; Grcić, J.; Nöth, H. *Z. Naturforsch.* **2004**, *59b*, 161–166.

Scheme 4. Synthesis of Bis(alkylzinc)-hydride-di(2-pyridylmethyl)amides (6−8)

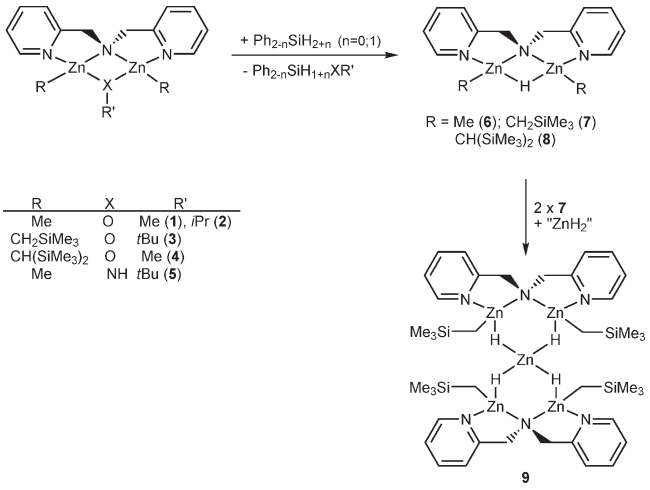

15 min a white solid precipitated from the reaction solution of **3** with $PhSiH_3$ or Ph_2SiH_2 in heptane. Recrystallization from a toluene/heptane mixture yielded colorless crystals suitable for X-ray structure analysis. Surprisingly a pentanuclear zinc hydride-bridged dimer $[\{Me_3SiCH_2Zn\}_4\{Zn(\mu\text{-}H)_4\}\{\mu\text{-}N(CH_2Py)_2\}_2]$ (**9**) crystallized instead of the initial dinuclear complex **7** (Scheme 3). Partial dismutation of **7** would lead to the intermediate formation of ZnH_2, which inserts into the strained four-membered Zn_2NH ring and concomitantly interconnects two equivalents of **7**. Homoleptic bis(trimethylsilylmethyl)zinc[28] as secondary coproduct of a dismutation process was detected in a considerable amount in the EI mass spectrum of **9**, supporting that the compound easily undergoes this reaction type. In the IR spectra of **9** no sharp Zn−H stretching frequencies are shown. Instead, broad absorptions are observed in the regions 1600−1300 and 1150−850 cm^{-1}, in contrast to the spectrum of **3**, indicating the presence of bridging hydrogen atoms.[3,13,16]

The hydride **9** crystallizes with two crystallographically independent molecules (distinguished with A and B) in the asymmetric unit. In Figure 2 only the molecular structure and numbering scheme of molecule A is depicted. The molecular structure of **9** is assembled from two six-membered $[\{Me_3SiCH_2Zn\}_2\{Zn(\mu\text{-}H)_2\}\{\mu\text{-}N(CH_2Py)_2\}]$ rings fused at Zn1. Each ring adopts a shallow skew-boat conformation, as was also observed for the spirocyclic pentahydride **I**.[13] The ring expansion with an additional Zn−H unit and hydride coordination to zinc has

Scheme 5. Reactivity of Bis(methylzinc)-hydride-di(2-pyridylmethyl)amide (6)

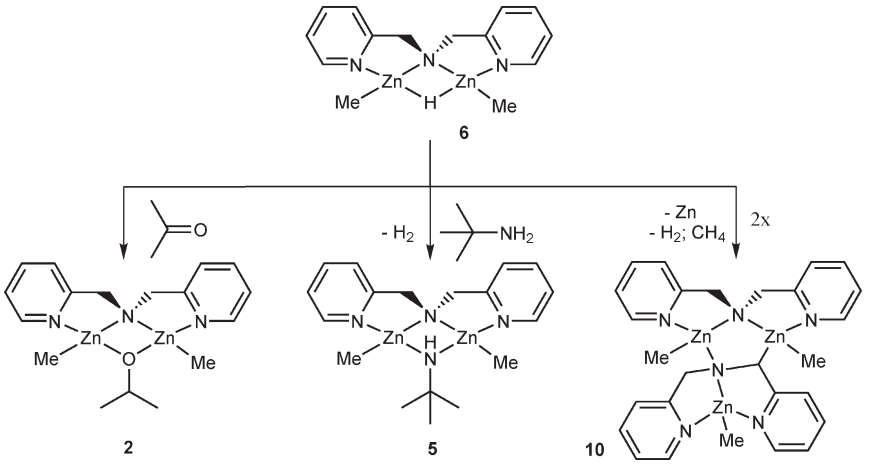

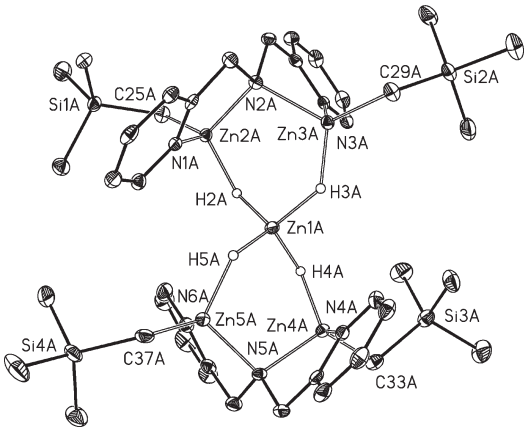

Figure 2. Molecular structure and numbering scheme of **9**. The hydrogen atoms with the exception of the bridging hydrides are omitted for clarity. The ellipsoids of all non-hydrogen atoms represent a probability of 40%. Selected bond lengths (pm) and angles (deg): Zn−N_{py} 212.6(3)−216.3(3), Zn−(μ-N) 204.8(3)−205.6(3), Zn−C 199.6(3)− 199.9(3), Zn1A−H2A 163(3), Zn1A−H3A 174(3), Zn1A−H4A 161(3), Zn1A−H5a 166(5), Zn2−H2A 176(3), Zn3A−H3A 167(4), Zn4A−H4A 172(4), Zn5A−H5A 175(4); H2A−Zn1A−H3A 110.9(2), H2A−Zn1A−H4A 108.0(2), H2A−Zn1A−H5A 109.7(2), H3A−Zn1A−H4A 108.9(2), H3A−Zn1A−H5A 107.8(2).

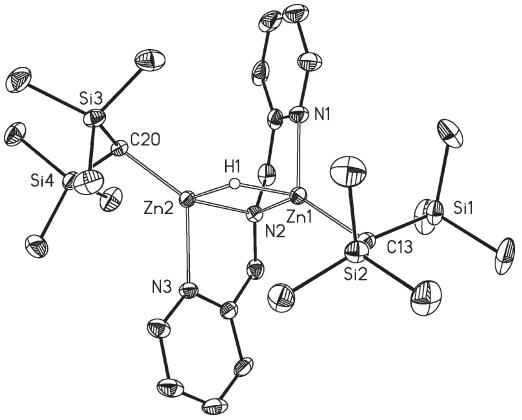

Figure 3. Molecular structures and numbering schemes of **8**. The hydrogen atoms with the exception of the bridging hydride are omitted for clarity. The ellipsoids of all non-hydrogen atoms represent a probability of 40%.

hardly any effect on the Zn−N2/N_{py} and Zn−C bond lengths compared to **3**. Adopting an almost ideal tetrahedral symmetry, the central zinc atom Zn1 may be regarded as a tetrahydrido zincate dianion (ZnH_4^{2-}), as found in $M_2[ZnH_4]$ and $M_3[ZnH_4(H)]$[31] chelated by two $[\{Me_3SiCH_2Zn\}_2\{\mu\text{-}N(CH_2Py)_2\}]^+$ cations.

The average Zn−H bond length in the tetrahydrido zincate (166(3) pm) was found to be slightly shorter than the outer Zn−H distances (average Zn−H 173 pm) and also compared to the similar fragment of complex **I** (176(4) pm).

The reaction of **4** with phenylsilane led to an exchange of the bridging alkoxide group against a hydride and yielded **8**, which immediately deposited as large colorless prisms from the reaction mixture. Despite missing sharp Zn−H stretching frequencies, the IR spectra of **8** again features broad underlying absorptions in the region 1200−950 and 800−600 cm^{-1}, which are attributable to a Zn-(μ-H) moiety.[3,13,16] An X-ray structure determination confirmed the presence of a hydride bridging the distorted tetrahedrally coordinated zinc centers. The molecular structure and numbering scheme of **8** are shown in Figure 3. The exchange of the alkoxide by a hydride does not lead to major changes for the Zn−N and Zn−C bonds lengths of the backbone (see Table 1). The shorter bond distance to the bridging hydride moiety causes a small Zn1−N2−Zn2 angle (78.9°) and a short transannular nonbonding Zn···Zn separation (262.1(1) pm) in the four-membered Zn_2NH ring.

Table 2 summarizes the calculated Zn−C bond lengths and the natural charges on zinc derived from natural orbital analysis for the monomeric hydrides **6**, **7**, and **8**. Similar to the alkoxide structures **2**, **3**, and **4** the metal−carbon bonds elongate with an increasing number of trimethylsilyl substituents, suggesting a weaker bond with a poorer carbon donor ability. As a consequence, compensation of the positive charge at the zinc atoms is diminished, which may lead to a loss of basicity of the attached hydride. Thus the hydride **6** features the shortest Zn−C bond and the most reactive hydride able to undergo intermolecular deprotonation. Silyl substituents lower this reactivity also for sterical reasons.

(31) (a) Bortz, M.; Yvon, K.; Fischer, P. J. *Alloys Compd.* **1994**, *216*, 39–42. (b) Bortz, M.; Yvon, K.; Fischer, P. J. *Alloys Compd.* **1994**, *216*, 43–45. (c) Bortz, M.; Hewat, A.; Yvon, K. J. *Alloys Compd.* **1997**, *248*, L1–L4. (d) Bortz, M.; Hewat, A.; Yvon, K. J. *Alloys Compd.* **1997**, *253−254*, 13–16.

Table 2. Selected Experimental and Calculated Bond Lengths (pm) and Natural Atomic Charges for 6, 7, and 8 Calculated at the B3LYP/TZVP//ECP-10-MDF Level of Theory

	bond lengths [pm]		
structure	$Zn-CH_{n=1-3}$ (exptl)	$Zn-CH_{n=1-3}$ (calcd)	natural atomic charge on Zn [*e*]
6		202.2/202.2	1.39/1.39
7		203.1/203.1	1.41/1.42
8	199.7(3)/200.3(3)	205.2/205.3	1.47/1.48

Table 3. NMR Chemical Shifts (ppm) Measured in C_6D_6 at 30 °C for the Compounds 2−4, 6, 8, and 9

δ	**2**	**3**	**4**	**6**	**9**	**8**
^{1}H						
Pyr 1	8.11	8.20	8.22	8.08	8.31	8.19
Pyr 2	6.45	6.49	6.53	6.42	6.56	6.48
Pyr 3	6.88	6.90	6.91	6.84	6.87	6.87
Pyr 4	6.66	6.75	6.73	6.58	6.65	6.66
CH_2N	4.16	4.22	4.24	4.06	4.07	4.30
$ZnCH_{n=1-3}$	−0.37	−0.76	−1.24	−0.44	−0.90	−1.37
μ-H				4.83	3.75	5.30
$SiMe_3$		0.09	0.13		0.12	0.10
^{13}C						
Pyr 1	147.1	146.4	147.5	147.9	148.0	147.4
Pyr 2	122.4	121.8	122.7	122.4	122.7	122.9
Pyr 3	137.6	137.1	138.1	137.7	138.0	138.1
Pyr 4	121.1	121.7	122.9	122.1	122.4	122.4
Pyr 5	161.7	160.4	160.8	161.9	161.5	160.7
CH_2N	60.6	59.8	59.7	60.8	60.6	60.4
$SiMe_3$		2.8	4.7		3.6	4.4
$ZnCH_{n=1-3}$	−16.9	−8.2	−3.0	−15.2	−8.3	−3.0

The design of the spectator alkyl ligands seems to be an effective tool in order to adjust reactivity.

NMR Investigations. The NMR data of the compounds **2**−**4**, also of **6**, **8**, and **9** (see Table 3), show characteristic trends. The pyridyl and methylene resonances of the side arm slightly shift downfield in the ^{1}H NMR spectra (C_6D_6) with an increasing number of trimethylsilyl substituents at the zinc-bound carbon atom. The trimethylsilyl resonances also shift to lower field, whereas the proton signal at the α-carbon experiences a remarkably high-field shift with an increasing degree of trimethylsilyl substitution. Both findings are in agreement with the observations made for the homologous row of homoleptic $Zn[CH_{3-n}(SiMe_3)_n]_2$.[28] In comparison to the proton resonances of the alkoxides **2**−**4** the chemical shifts of the pyridyl protons and the proton signals of the organometallic group in the hydrides **6**, **8**, and **9** are detected at higher field. The chemical shifts of the hitherto isolated zinc hydrides vary in a range from 4.39[6] to 5.36 ppm[5] independent of a terminal or a bridging coordination mode. Therefore the hydride resonance in complex **9** lies in an unusually high field, which may to some degree reflect the "ate" nature[15] of the central fragment. However, the chemical shift of the related structure **I** with a tetrahydrido zincate unit was found at δ = 5.10 ppm.[13]

In the ^{13}C NMR spectrum a strong correlation between the number of trimethylsilyl substituents and the deshielding of the metal-bound carbon is observed for all complexes. Similarly, the signal of the trimethylsilyl groups itself shifts slightly downfield with an increasing number of trimethylsilyl groups. When going from alkoxide to hydride coordination, the chemical shifts of the zinc-bound carbon and the trimethylsilyl groups remain almost unchanged.

Catalytic Investigations. The conversion of the alkoxides **1**−**4** into a hydride (Scheme 4) and vice versa (Scheme 5)

Scheme 6. Zinc-Catalyzed Hydrosilylation of Acetone and Benzaldehyde with Diphenylsilane

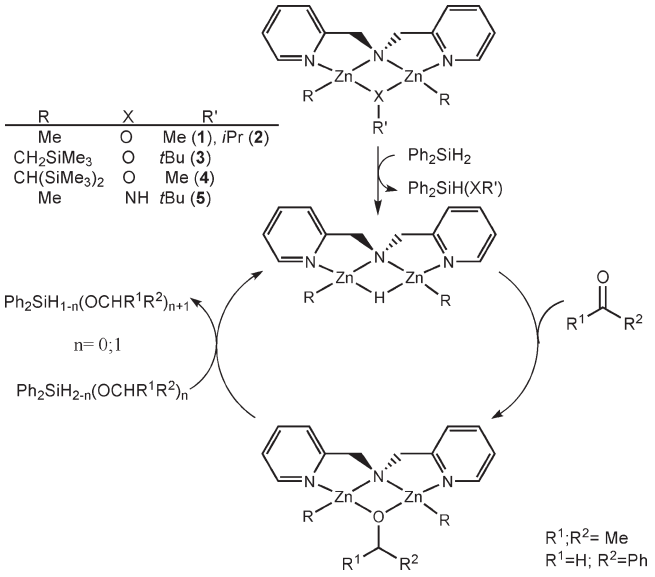

suggests the development of a catalytic cycle for hydrosilylation, yielding silyl ethers from aldehydes and ketones. Besides complex **2** also the amide **5** and zinc alkoxide **1** showed a comparable catalytic activity in this process (see Scheme 6).

In a typical experiment two equivalents of acetone or benzaldehyde were reacted with diphenylsilane at room temperature using catalyst **1** or **2** with a concentration of 3 mol %. The reactions were monitored by ^{1}H NMR spectroscopy and showed the complete absence of the silicon-bound proton resonance after less than 30 min and after 15 min in the case of the aldehyde. When phenylsilane was used, the reactions proceeded even faster, indicating the strong influence of the steric requirements of the silane as the rate-limiting factor. For this reason no conversion was observed with triethylsilane. Even traces of water in the presence of arylsilanes were tolerated by the catalyst, converting them to polydiphenylsiloxane and hydrogen.

Attempts to follow the catalyst behavior of **2** by ^{1}H NMR spectroscopy employing a detectable amount (5−10 mol %) of the catalyst failed due to the rapidness of the reaction. The lowered reactivity of the bulkier zinc alkoxides **3** and **4** makes them more appropriate for this purpose. In a NMR-scale experiment the hydrosilylation of acetone with diphenylsilane catalyzed by 5 mol % of **3** and **4** was monitored after 30 min and three hours (see Figure 4). As expected, the reaction rate decreases with increasing trimethylsilyl substitution at the organometallic carbon. After three hours one equivalent of acetone was added to diphenylsilane when catalyzed by **3**, whereas the resonances of diphenylsilane have not completely vanished in the catalysis with **4**. In contrast to catalyst **2** the formed $Ph_2SiH(OCHMe_2)$ is not able to add a second equivalent of acetone as a result of the steric shielding of the catalysts **3** and **4**. Looking at the catalyst itself, the pyridyl resonances are almost identical to those found for the alkoxides **3** and **4** (cf. Table 3), suggesting that the isopropoxide form of the catalyst is more stable than the hydride forms **7** and **8**.

Theoretical Studies. In order to gain a detailed picture of the mechanistic aspects of the hydrosilylation of aldehydes and ketones, catalyzed by a dinuclear zinc species, extensive density functional theoretical calculations were carried out.

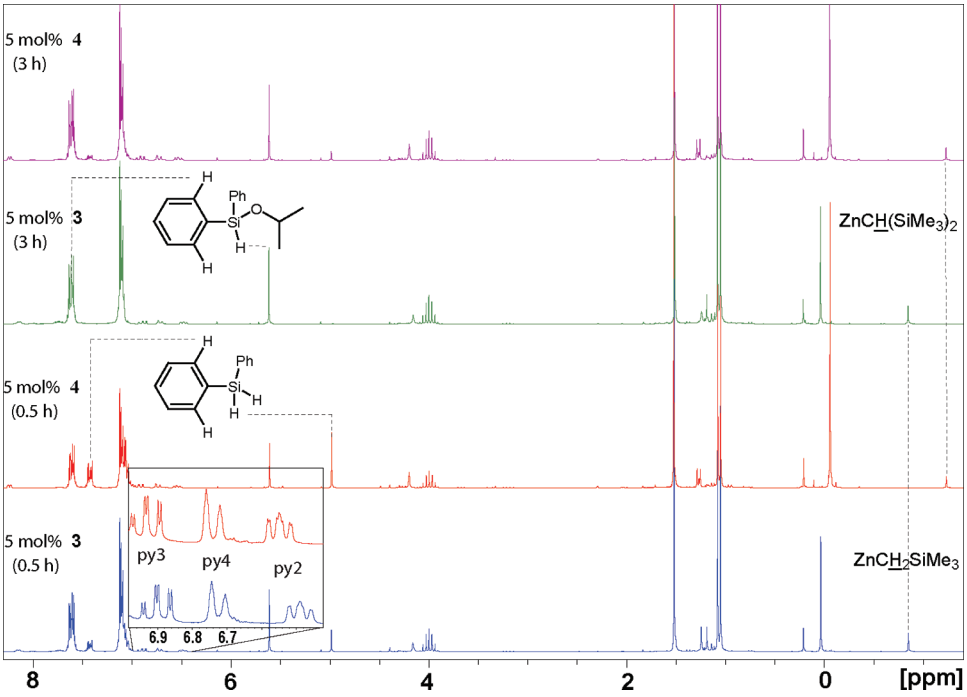

Figure 4. ^{1}H NMR studies on the hydrosilylation reaction of acetone with diphenylsilane catalyzed by 5 mol % of **3** and **4**.

In analogy to the experiments the reaction of acetone with phenylsilane was investigated as an appropriate reference system. The catalyst itself was modeled by the zinc hydride **6**, which showed the fastest conversion rates. The overall reaction proceeds in an exergonic way with a calculated reaction Gibbs free energy $\Delta_R G$ of −12.2 kcal/mol (eq 1). The Gibbs free energies of stationary points on the potential energy surfaces are listed in Table 4. In addition, Figure 5 provides an energetic representation of the reaction profile. Note that the entropy contributing to the Gibbs free energy arises from the assumption that all substrates are treated as ideal gases. In the gas phase entropy grows mostly in its translation and rotation components, but this reaction is carried out in solution and the translation and rotation movements are limited. Therefore, the ΔG value is regarded to be smaller than the calculated one.[32]

$$\mathrm{PhSiH_3 + Me_2C{=}O \rightarrow PhSiH_2(OCHMe_2)}$$
$$\Delta_R G = -12.2\ \mathrm{kcal/mol} \qquad (1)$$

$$\mathbf{6} + \mathrm{Me_2CO} \rightarrow \mathbf{2}$$
$$\Delta_R G = -17.2\ \mathrm{kcal/mol} \qquad (2)$$

$$\mathbf{2} + \mathrm{PhSiH_3} \rightarrow \mathbf{6} + \mathrm{PhSiH_2(OCHMe_2)}$$
$$\Delta_R G = 5.0\ \mathrm{kcal/mol} \qquad (3)$$

The catalytic cycle is represented in Scheme 7 and can be regarded as a two-step reaction. The first reaction is the conversion of hydride **6** into the alkoxide **2** via addition of acetone (eq 2), and the second step is the recovery of hydride **6** from **2** by its reaction with phenylsilane (eq 3). The addition of acetone to starting hydride **6** proceeds very rapidly and under remarkable warming of the reaction mixture. Quantum chemical investigations show that acetone approaches from the less hindered side forming the weak adduct **E1** with a loose hydrogen bond, this adduct is destabilized by 7.9 kcal/mol^{-1} with respect to the reactants. In this complex the ketone is perfectly aligned to approach one of the Lewis acidic zinc ions. The coordination of the acetone molecule at zinc weakens (**TS1**) and finally breaks the Zn(μ-H)Zn bridge (**I1**). In this dinuclear complex the amide nitrogen atom bridges both zinc atoms which are in significantly different environments. One zinc atom carries the acetone ligand, which still exhibits a characteristic C=O double bond. The other zinc atom can be regarded as a Me−Zn−H molecule coordinated by a bidentate pyridylmethylamido chelate base. The acetone ligand approaches the other zinc atom to an increasing degree which leads to an elongation of the Zn−H bond and a rather short distance to the ketone carbon atom (**TS2**). This transition state is 29.2 kcal/mol^{-1} higher in energy than the initial starting materials and a relaxation to isopropoxide **2** occurs immediately. This complex **2** possesses a planar central Zn_2NO ring with an oxygen atom in

Table 4. Gibb's Free Energies [kcal/mol] of the Hydrosilylation Reaction, Calculated at the B3LYP/TZVP//ECP-10-MDF Level of Theory[a]

structure	ΔG	structure	ΔG
6 + Me_2CO + $PhSiH_3$	0.0	**E2**	−11.4
E1 + $PhSiH_3$	7.9	**TS3**	21.7
TS1 + $PhSiH_3$	18.6	**I2**	20.0
I1 + $PhSiH_3$	17.6	**TS4**	23.3
TS2 + $PhSiH_3$	29.2	**I3**	15.3
2 + $PhSiH_3$	−17.2	**TS5**	16.3
		E3	−3.3
		6 + $PhSiH_2OCHMe_2$	−12.2

[a] The values are given relative to **6** plus free acetone and $PhSiH_3$ molecule.

(32) (a) Tamura, H.; Yamazaki, H.; Sato, H.; Sakaki, S. *J. Am. Chem. Soc.* **2003**, *125*, 16114–16126. (b) Sakaki, S.; Takayama, T.; Sumimoto, M.; Sugimoto, M. *J. Am. Chem. Soc.* **2004**, *126*, 3332–3348. (c) Sumimoto, M.; Takahama, N. I. T.; Sakaki, S. *J. Am. Chem. Soc.* **2004**, *126*, 10457–10471. (d) Braga, A. A. C.; Ujaque, G.; Maseras, F. *Organometallics* **2006**, *25*, 3647–3658. (e) Deglmann, P.; Ember, E.; Hofmann, P.; Pitter, S.; Walter, O. *Chem.—Eur. J.* **2007**, *13*, 2864–2879.

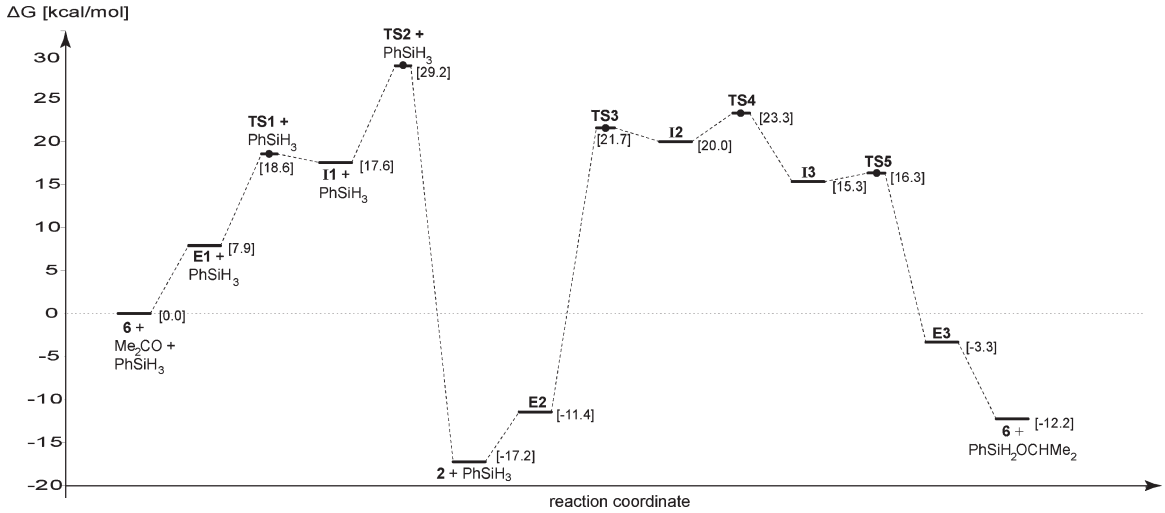

Figure 5. Energy diagram of the zinc-catalyzed hydrosilylation of acetone with phenylsilane, calculated at the B3LYP/TZVP//ECP-10-MDF level of theory. The values are given in kcal/mol relative to **6**, a free acetone and a phenylsilane molecule. The optimized structures can be found in the Supporting Information.

Scheme 7. Calculated Pathway of the Hydrosilylation of Acetone with Phenylsilane[a]

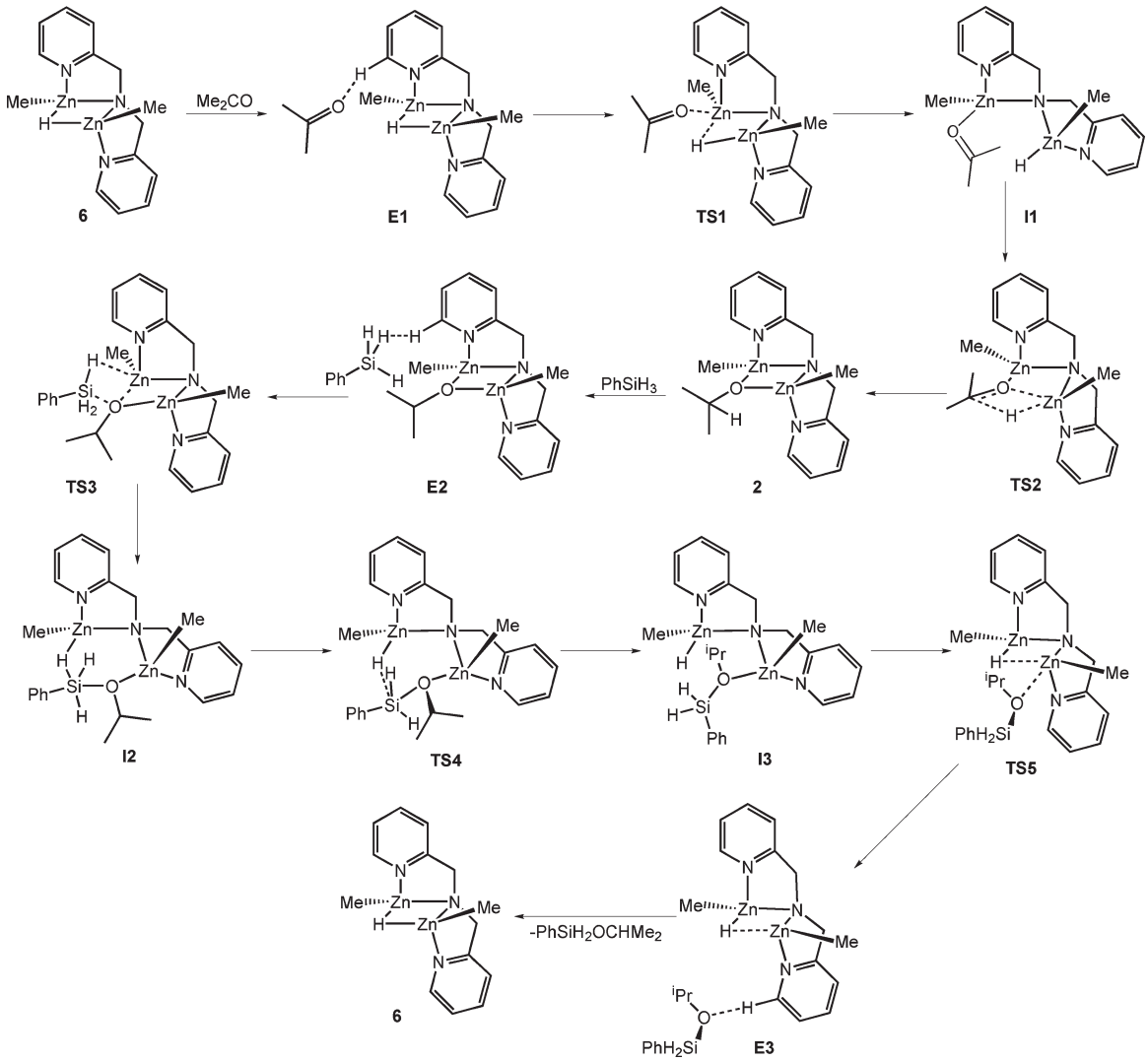

[a] The optimized structures, calculated at the B3LYP/TZVP//ECP-10-MDF level of theory, can be found in the Supporting Information. The corresponding Gibbs free energies are summarized in Table 4.

a distorted trigonal-planar environment and represents the most stable species in the catalytic cycle ($\Delta G = -17.2$ kcal/mol^{-1}).

The phenylsilane molecule approaches the dinuclear zinc complex (**E2**) forming a weak Zn(μ-H)Si hydride bridge to one zinc atom, which weakens the Zn−O bond simultaneously (**TS3**). Finally this Si−H moiety inserts into the Zn−O bond leading to a six-membered Zn_2NOSiH ring with a bridging $PhSi(H)_3(OCHMe_2)$ anion (**I2**), which contains a pentacoordinate silicon atom. Breakage of the Si−H bond (**TS4**) and reorientation of this dinuclear intermediate leads to **I3** with a Me−Zn−H fragment trapped by the chelate pyridylmethylamido base. In intermediate **I3** the oxygen atom is in a nearly trigonal planar environment with a rather large Zn−O distance. The zinc hydride still shows a weak electrostatic attraction to the electropositive silicon atom. Such electrostatic bonding situations between Lewis acidic metal ions and silanes have already been observed for tantalum, niobium[33] and ruthenium complexes.[34] Closure of the Zn_2NH ring and release of phenylsilyl isopropylether regain **6** via the transition state **TS5**.

Summary and Conclusions

Bis(alkylzinc)-hydride-di(2-pyridylmethyl)amides {alkyl = Me (**6**), CH_2SiMe_3 (**7**), $CH(SiMe_3)_2$ (**8**)} were synthesized by a straightforward procedure from the corresponding alkoxides. However, the methyl derivative **6** decomposes within a few hours. Stability is enhanced for the more shielded complex **7**, but this compound converts to a pentanuclear zinc complex **9** with a tetrahydridozincate anion. Steric protection by bis(trimethylsilyl)methyl groups leads to a stable bis(alkylzinc)-hydride-di(2-pyridylmethyl)amide. These compounds effectively catalyze the hydrosilylation of aldehydes and ketones. The rate strongly depends on the bulkiness of the alkyl group. NMR investigations on the catalysis identify the alkoxides to be the energetically most favored species and show that the regeneration of the hydride depends on the nature of the silane. Density functional theoretical calculations confirm the rate-limiting step to be the formation of the silyl ether concomitant with the regeneration of the hydride species. The experimental and theoretical findings provide a complete mechanistic picture of the hydrosilylation reaction catalyzed by a dinuclear zinc catalyst. Also the role of the two catalytic centers in a close nonbonding distance is clarified for the hydride transfer, one zinc ion being in the role of substrate fixation and activation whereas an alkylzinc hydride species is generated in situ on the cocatalytic second center. These observed synergetic effects might also be relevant in dinuclear transferases. Control of the reactivity by electronic and steric means in case of **3** and **4** builds a promising base for highly enantioselective catalysis.

Experimental Section

General Remarks. All manipulations were carried out under an argon atmosphere using standard Schlenk techniques. The solvents were dried according to common procedures and distilled under argon; deuterated solvents were dried over sodium, degassed, and saturated with argon. Acetone, 2-propanol, and benzaldehyde were dried over activated 4 Å molecular sieves and destilled under argon prior to use. The compounds $[(MeZn)_2(\mu\text{-OMe})\{\mu\text{-N}(CH_2Py)_2\}]$ (**1**), $[\{(Me_3Si)_2CHZn\}_2(\mu\text{-OMe})\{\mu\text{-N}(CH_2Py)_2\}]$ (**4**), and $[(MeZn)_2(\mu\text{-N(H)tBu})\{\mu\text{-N}(CH_2Py)_2\}]$ (**5**) were prepared by a previously published procedure.[26] All other compounds were used as supplied by the manufacturer.

The ^{1}H and $^{13}C\{^1H\}$ NMR spectra were recorded on a Bruker AC 400 MHz spectrometer. Mass spectra were obtained on a Finnigan MAT SSQ 710 system, and IR measurements were carried out using a Perkin-Elmer System 2000 FTIR. The IR spectra were taken as Nujol mulls between KBr windows. Melting and decomposition points were measured with a Stuart apparatus type SMP3 and are uncorrected. For the elemental analysis V_2O_5 was added to the samples in order to enhance combustion; nevertheless, carbon values are low, most probably due to carbonate formation during combustion.

Synthesis of $[(MeZn)_2(\mu\text{-OCHMe}_2)\{\mu\text{-N}(CH_2Py)_2\}]$ (2). Procedure A. A mixture of di(2-pyridylmethyl)amine (0.60 g, 3.0 mmol) and 2-propanol (0.18 g, 3.0 mmol) was dissolved in toluene (15 mL) and cooled to −78 °C. To the stirred solution a 1.2 M solution of dimethylzinc in toluene (5.0 mL, 6.0 mmol) was added dropwise. The reaction mixture turned claret red while methane was slowly liberated. After being warmed to rt the solution was stirred for additional 14 h. The volume of the solution was reduced to two-thirds of the original volume. Cooling of this solution to 5 °C led to the precipation of colorless crystals of **2**. Yield: 0.95 g, 76%.

Procedure B. The freshly prepared solution of **6**, according to the below procedure, was reacted with acetone (80 μL, 1.1 mmol), which was added dropwise to the stirred mixture. In the course of the reaction a slight warming was observed. After being stirred for an additional hour, the volume of the solution was reduced under vacuum to half of the original volume. Cooling of this solution to −20 °C led to the immediate precipitation of amorphous **2**. Recrystallization from toluene gave **2** as colorless prisms. Yield: 0.19 g, 91%.

Physical Data of 2. Decomposition above 128 °C. Anal. Calcd for $C_{17}H_{25}N_3OZn_2$ (418.18): C 48.83, H 6.03, N 10.50. Found: C 46.66, H 5.74, N 9.80. ^{1}H NMR (400.25 MHz, C_6D_6, 300 K): δ −0.37 (s, 6H, $ZnCH_3$), 1.35 (d, $^3J_{H-H}$ = 6.0 Hz, 6H, $CH(\underline{CH_3})_2$), 4.16 (s, 4H, CH_2N), 4.34 (hept, $^3J_{H-H}$ = 6.0 Hz, 1H, $\underline{CH}(CH_3)_2$), 6.45 (m, 2H, Pyr2), 6.66 (d, $^3J_{H-H}$ = 7.6 Hz, 2H, Pyr4), 6.88 (dt, $^3J_{H-H}$=7.6 Hz, $^4J_{H-H}$=1.6 Hz, 2H, Pyr3), 8.11 (d, $^3J_{H-H}$=4.8 Hz, 2H, Pyr1). $^{13}C\{^1H\}$ NMR (50.33 MHz, C_6D_6, 300 K): δ −16.9 ($ZnCH_3$), 29.3 ($CH(\underline{CH_3})_2$) 60.6 (CH_2N), 66.1 ($\underline{CH}(CH_3)_2$), 122.1 (Pyr4), 122.4 (Pyr2), 137.6 (Pyr3), 147.1 (Pyr1), 161.7 (Pyr5). MS (EI, m/z, [%]): 93 ($[C_6H_7N]^+$) [100], 200 ($[C_{12}H_{14}N_3]^+$) [74], 262 ($[C_{12}H_{12}N_3{}^{64}Zn]$) [55], 278 ($[C_{12}H_{12}N_3O^{64}Zn]$) [93], 342 ($[C_{12}H_{12}N_3O^{64}Zn_2]$) [21], 356 ($[M(^{64}Zn/^{64}Zn)\text{-OMe}]^+$) [27], 400 ($[M(^{64}Zn/^{64}Zn)\text{-}CH_3]^+$) [34]. IR (Nujol, KBr, cm^{-1}): ν 3174 m, 3058 m, 3017 m, 2920 vs, 2852 vs, 2743 m, 2703 m, 2676 m, 2611 m, 2263 w, 2167 w, 1992 w, 1953 w, 1910 w, 1885 w, 1843 w, 1716 w, 1650 m, 1602 s, 1593 s, 1570 s, 1457 vs, 1377 s, 1341 s, 1296 s, 1284 s, 1229 m, 1154 s, 1100 s, 1048 s, 1018 m, 976 s, 956 m, 829 m, 755 s, 727 s, 639 s, 546 s.

Synthesis of $[\{Me_3SiCH_2Zn\}_2(\mu\text{-O}t\text{Bu})\{\mu\text{-N}(CH_2Py)_2\}]$ (3). Di(2-pyridylmethyl)amine (0.60 g, 3.0 mmol) and *tert*-butanol (0.22 g, 3.0 mmol) were dissolved in 5 mL of toluene and cooled to −78 °C. To the stirred mixture a solution of bis(trimethylsilylmethyl)zinc (1.45 g, 6.0 mmol) in 5 mL of toluene was added dropwise. After being warmed to rt the solution was stirred for additional 14 h. The volume of the solution was reduced to a few milliliters. The oily residue was dissolved in 5 mL of heptane, followed by the complete evaporation of the solvent. The remaining semicrystalline solid was again dissolved in 2 mL of heptane. Cooling of this solution to 5 °C led to the precipation of large colorless crystals of **3**. Yield: 1.60 g, 78%.

(33) (a) Bakhmutov, V. I.; Howard, J. A. K.; Keen, D. A.; Kuzmina, L. G.; Leech, M. A.; Nikonov, G. I.; Vorontsov, E. V.; Wilson, C. C. *J. Chem. Soc., Dalton Trans.* **2000**, 1631–1635. (b) Nikonov, G. I.; Mountford, P.; Ignatov, S. K.; Green, J. C.; Leech, M. A.; Kuzmina, L. G.; Razuvaev, A. G.; Rees, N. H.; Blake, A. J.; Howard, J. A. K.; Lemenovskii, D. A. *J. Chem. Soc., Dalton Trans.* **2001**, 2903–2915. (c) Dubberley, S. R.; Ignatov, S. K.; Rees, N. H.; Razuvaev, A. G.; Mountford, P.; Nikonov, G. I. *J. Am. Chem. Soc.* **2003**, *125*, 642–643.

(34) Hussein, K.; Marsden, C. J.; Barthelat, J.-C.; Rodriguez, V.; Conejero, S.; Sabo-Etienne, S.; Donnadieu, B.; Chaudret, B. *Chem. Commun.* **1999**, 1315–1316.

Physical Data of 3. Melting point: 87 °C. Anal. Calcd for $C_{24}H_{43}N_3OSi_2Zn_2$ (576.57): C 50.00, H 7.52, N 7.29. Found: C 49.12, H 7.74, N 7.23. ^{1}H NMR (400.25 MHz, C_6D_6, 300 K): δ −0.76 (s, 4H, ZnC$\underline{H_2}$Si(CH$_3$)$_3$), 0.09 (s, 18H, CH$_2$Si(C$\underline{H_3}$)$_3$), 1.33 (s, 9H, C(CH$_3$)$_3$), 4.22 (s, 4H, CH$_2$N), 6.49 (m, 2H, Pyr2), 6.75 (d, $^3J_{H-H}$ = 7.6 Hz, 2H, Pyr4), 6.90 (dt, $^3J_{H-H}$ = 7.6 Hz, $^4J_{H-H}$ = 1.6 Hz, 2H, Pyr3), 8.22 (d, $^3J_{H-H}$ = 4.8 Hz, 2H, Pyr1). ^{13}C{^{1}H} NMR (50.33 MHz, C_6D_6, 300 K): δ −8.2 (Zn$\underline{C}$H$_2$Si(CH$_3$)$_3$), 2.8 (CH$_2$-Si($\underline{C}$H$_3$)$_3$), 34.0 (C($\underline{C}$H$_3$)$_3$), 59.8 (CH$_2$N), 68.7 ($\underline{C}$(CH$_3$)$_3$), 121.7 (Pyr4), 121.8 (Pyr2), 137.1 (Pyr3), 146.4 (Pyr1), 160.4 (Pyr5). MS (EI, m/z, [%]): 73 ([Si(CH$_3$)$_3$]$^+$/[C$_4$H$_9$O]$^+$) [100], 93 ([C$_6$H$_7$N]$^+$) [81], 200 ([C$_{12}$H$_{14}$N$_3$]$^+$) [12], 262 ([C$_{12}$H$_{12}$N$_3$^{64}Zn]) [14], 334 ([C$_{15}$H$_{20}$N$_3$Si^{64}Zn]) [3.7], 490 ([M(^{64}Zn/^{64}Zn)-CH$_2$SiMe$_3$]$^+$)[5.8], 560 ([M(^{64}Zn/^{64}Zn)-CH$_3$]$^+$) [0.2]. IR (Nujol, KBr, cm^{-1}): ν 3176 m, 3100 m, 3025 m, 3017 m, 2922 vs, 2853 vs, 2740 m, 2699 m, 2675 m, 2621 m, 2306 w, 2253 w, 2163 w, 1996 w, 1981 w, 1953 w, 1910 m, 1881 w, 1838 m, 1756 w, 1714 w, 1651 m, 1605 s, 1572 s, 1521 w, 1455 vs, 1377 s, 1353 s, 1284 s, 1237 vs, 1201 vs, 1152 s, 1123 s, 1100 s, 1048 s, 1019 m, 1008 m, 976 s, 923 vs, 857 vs, 820 vs, 754 vs, 678 s, 641 m, 606 m, 575 s 553 s, 506 s, 467 s.

Synthesis of [(MeZn)$_2$(μ-H){μ-N(CH$_2$Py)$_2$}] (6). Diphenylsilane (0.10 g, 0.5 mmol) was added dropwise to a solution of [(MeZn)$_2$(μ-N(H)tBu){μ-N(CH$_2$Py)$_2$}] (**5**) (0.22 g, 0.5 mmol) or [(MeZn)$_2$(μ-OMe){μ-N(CH$_2$Py)$_2$}] (**1**) (0.21 g, 0.5 mmol) in [D$_8$]toluene (3.0 mL). The reaction progress was followed by ^{1}H NMR spectroscopy, showing complete conversion after 15 min. When stored at −20 °C the pale yellow solution turned deep orange within days, indicating the slow degradation of the zinc hydride **6**. Thus all attemps for crystallization yielded the degradation product **10**. Nevertheless, **6** is stable in solution for a couple of hours. Physical data of **6**: ^{1}H NMR (400.25 MHz, C_6D_6, 300 K): δ −0.44 (s, 6H, ZnCH$_3$), 4.06 (s, 4H, CH$_2$N), 4.83 (s, 1H, ZnH), 6.42 (m, 2H, Pyr2), 6.58 (d, $^3J_{H-H}$ = 7.6 Hz, 2H, Pyr4), 6.84 (t, $^3J_{H-H}$ = 7.6 Hz, 2H, Pyr3), 8.08 (s (br), 2H, Pyr1). ^{13}C{^{1}H} NMR (100.65 MHz, C_6D_6, 300 K): δ −15.2 (ZnCH$_3$), 60.8 (CH$_2$N), 122.1 (Pyr4), 122.4 (Pyr2), 137.7 (Pyr3), 147.9 (Pyr1), 161.9 (Pyr5).

Synthesis of [{(Me$_3$Si)$_2$CHZn}$_2$(μ-H){μ-N(CH$_2$Py)$_2$}] (8). To a stirred solution of [{(Me$_3$Si)$_2$CHZn}$_2$(μ-OMe){μ-N(CH$_2$-Py)$_2$}] (**4**) (1.00 g, 1.47 mmol) in heptane (12 mL) phenylsilane (0.22 g, 2.0 mmol) was added dropwise. Storage of this solution at rt led to the immediate precipitation of large colorless prisms, which were collected. Concentration of the mother liquor under vacuum and storage at 5 °C afforded a further crop of crystals of **8**. Yield: 0.84 g, 88%. Physical data of **8**: Decomposition above 110 °C. Anal. Calcd for $C_{26}H_{51}N_3Si_4Zn_2$ (648.83): C 48.13, H 7.92, N 6.48. Found: C 47.85, H 8.04, N 6.23. ^{1}H NMR (400.25 MHz, C_6D_6, 300 K): δ −1.37 (s, 2H, ZnC$\underline{H}$(Si(CH$_3$)$_3$)$_2$), 0.10 (s, 36H, CH(Si(C$\underline{H_3}$)$_3$)$_2$), 4.30 (s, 4H, CH$_2$N), 5.30 (s, 1H, ZnH), 6.48 (m, 2H, Pyr2), 6.66 (d, $^3J_{H-H}$ = 7.6 Hz, 2H, Pyr4), 6.87 (dt, $^3J_{H-H}$ = 7.6 Hz, $^4J_{H-H}$ = 1.6 Hz, 2H, Pyr3), 8.19 (d, $^3J_{H-H}$ = 4.8 Hz, 2H, Pyr1). ^{13}C{^{1}H} NMR (100.65 MHz, C_6D_6, 300 K): δ −3.0 (Zn$\underline{C}$H(Si(CH$_3$)$_3$)$_2$), 4.4 (CH(Si($\underline{C}$H$_3$)$_3$)$_2$), 60.4 (CH$_2$N), 122.4 (Pyr4), 122.9 (Pyr2), 138.1 (Pyr3), 147.4 (Pyr1), 160.7 (Pyr5). MS (EI, m/z, [%]): 129 ([C$_5$H$_{13}$Si$_2$]$^+$) [100], 262 ([C$_{12}$H$_{12}$N$_3$^{64}Zn]$^+$) [83], 486 ([M(^{64}Zn/^{64}Zn)-CH(SiMe$_3$)$_2$]$^+$) [66], 644 ([M(^{64}Zn/^{64}Zn)-H]$^+$) [4]. IR (Nujol, KBr, cm^{-1}): ν 3100 m, 3059 m, 2922 vs, 2852 vs, 2738 m, 2698 m, 2671 m, 2622 w, 2308 w, 2258 w, 2206 w, 2110 w, 1994 w, 1955 w, 1912 m, 1881 w, 1840 m, 1714 w, 1645 w, 1606 s, 1569 m, 1463 vs, 1378 s, 1341 m, 1283 m, 1239 s, 1153 m, 1130 m, 1101 m, 1049 m, 1019 s, 981 m, 848 vs, 830 vs, 755 vs, 667 s, 641 m, 605 s, 490 m.

Synthesis of [{Me$_3$SiCH$_2$Zn}$_4${Zn(μ-H)$_4$}{μ-N(CH$_2$Py)$_2$}$_2$] (9). To a stirred solution of [{Me$_3$SiCH$_2$Zn}$_2$(μ-OtBu){μ-N-(CH$_2$Py)$_2$}] (**3**) (0.32 g, 0.55 mmol) in heptane (6 mL) was added dropwise phenylsilane (70 μL, 0.57 mmol). After an induction phase of 15 min a cloudy white solid precipitated. The solid (0.24 g, 81%) was collected and washed with small amounts of heptane. Recrystallization from a toluene/heptane mixture and storage at 5 °C afforded **9** as colorless needles. Yield: 0.21 g, 71%. Physical data of **9**: Decomposition above 125 °C. Anal. Calcd for $C_{40}H_{72}N_6Si_4Zn_5$ (1076.33): C 44.64, H 6.74, N 7.81. Found: C 43.85, H 6.98, N 7.37. ^{1}H NMR (400.25 MHz, C_6D_6, 300 K): δ −0.90 (s, 8H, ZnC$\underline{H_2}$(Si(CH$_3$)$_3$)), 0.12 (s, 36H, CH$_2$(Si(C$\underline{H_3}$)$_3$)), 3.75 (s, 4H, ZnH), 4.07 (s, 8H, CH$_2$N), 6.56 (m, 4H, Pyr2), 6.65 (d, $^3J_{H-H}$ = 7.6 Hz, 4H, Pyr4), 6.87 (dt, $^3J_{H-H}$ = 7.6 Hz, $^4J_{H-H}$ = 1.6 Hz, 4H, Pyr3), 8.31 (d, $^3J_{H-H}$ = 4.8 Hz, 4H, Pyr1). ^{13}C{^{1}H} NMR (100.65 MHz, C_6D_6, 300 K): δ −8.3 (Zn$\underline{C}$H$_2$(Si(CH$_3$)$_3$)$_2$), 3.6 (CH(Si($\underline{C}$H$_3$)$_3$)), 60.6 (CH$_2$N), 122.4 (Pyr4), 122.7 (Pyr2), 138.0 (Pyr3), 148.0 (Pyr1), 161.5 (Pyr5). MS (EI, m/z, [%]): 73 ([C$_3$H$_9$Si]$^+$) [40], 93 ([C$_6$H$_7$N]$^+$) [11], 129 ([C$_5$H$_{13}$Si$_2$]$^+$) [100], 223 ([^{64}Zn(CH$_2$SiMe$_3$)$_2$-CH$_3$]$^+$) [40], 238 ([^{64}Zn(CH$_2$SiMe$_3$)$_2$]$^+$) [9], 414 ({R^{64}Zn}$_2$(μ-H){μ-N(CH$_2$Py)$_2$}-R]$^+$) [3.4], 486 ({R^{64}Zn}$_2$(μ-H){μ-N(CH$_2$Py)$_2$}-CH$_3$]$^+$) [0.5], 500 ({R^{64}Zn}$_2${μ-N(CH$_2$Py)$_2$}]$^+$) [0.3]. IR (Nujol, KBr, cm^{-1}): ν 3062 m, 2922 vs, 2852 vs, 2790 s, 2736 m, 2670 w, 2454 w, 2310 w, 2259 w, 2153 w, 1993 w, 2010 w, 1957 w, 1911 m, 1881 w, 1842 m, 1771 w, 1715 w, 1651 m, 1605 s, 1570 s, 1560−1470 s, 1455 vs, 1377 s, 1339 s, 1284 s, 1249 m, 1234 s, 1213 m, 1153 m, 1122 s, 1101 s, 1050 m, 1034 m, 1022 m, 1012 m, 981 m, 912 vs, 856 vs, 815 vs, 759 vs, 721 vs, 674 s, 641 m, 603 m, 547 s 495 s, 444 s.

Catalytic Hydrosilylation Reactions. In a typical experiment diphenylsilane (0.56 g, 3.0 mmol) and [(MeZn)$_2$(μ-OR){μ-N-(CH$_2$Py)$_2$}] (**1** or **2**) (35−40 mg, 0.09 mmol, 3 mol %) were dissolved in [D$_6$]benzene (3.0 mL). To the stirred solution was added dropwise the carbonyl compound (3.0 mmol). The progress of the reaction was monitored by ^{1}H NMR spectroscopy. After complete conversion the solvent was removed under vacuum and the crude product was distilled in a Kugelrohr.

Ph$_2$Si(OCH(CH$_3$)$_2$)$_2$ (11). Reaction completeness was detected by the absence of the SiH$_2$ resonances after 30 min. Kugelrohr distillation (160 °C, 5 × 10^{-2} mbar) gave a colorless oil. Yield: 0.79 g, 88%. The yield was diminished by small amounts of water in the acetone, which converted some of the diphenylsilane to polydiphenylsiloxane and hydrogen. Physical data of **11**: ^{1}H NMR (400.25 MHz, C_6D_6, 300 K): δ 1.14 (d, $^3J_{H-H}$ = 6.0 Hz, 12H, CH(C$\underline{H_3}$)$_2$), 4.17 (hept, $^3J_{H-H}$ = 6.0 Hz, 2H, C$\underline{H}$(CH$_3$)$_2$), 7.15−7.20 (m, 6H, m/p-Ph), 7.77−7.81 (m, 4H, o-Ph). ^{13}C{^{1}H} NMR (100.65 MHz, C_6D_6, 300 K): δ 25.9 (OCH($\underline{C}$H$_3$)$_2$), 66.0 (O$\underline{C}$H(CH$_3$)$_2$), 128.2 (m-Ph), 130.2 (p-Ph), 134.8 (i-Ph), 135.4 (o-Ph). MS (EI, m/z, [%]): 139 ([C$_6$H$_7$O$_2$Si]$^+$) [66], 181 ([C$_9$H$_{13}$O$_2$Si]$^+$) [40], 199 ([C$_{12}$H$_{11}$OSi]$^+$) [76], 222 ([M − C$_6$H$_6$]$^+$) [100], 241 ([M − OiPr]$^+$) [50], 285 ([M − CH$_3$]$^+$) [16], 300 ([M]$^+$) [10]. IR (film, KBr, cm^{-1}): ν 3069 m, 3050 m, 3002 m, 2972 s, 2931 s, 2890 s, 1960 w, 1891 w, 1825 w, 1777 w, 1592 w, 1464 m, 1451 m, 1429 s, 1381 s, 1369 s, 1305 w, 1264 w, 1224 w, 1173 s, 1115 vs, 1034 vs, 998 s, 886 m, 874 m, 762 m, 729 vs, 716s, 700 s, 579 w, 526 vs, 488 m.

Ph$_2$Si(OCH$_2$Ph)$_2$ (12). Reaction completeness was detected by the absence of the SiH$_2$ and CHO resonances after 15 min. Kugelrohr distillation (220 °C, 3.6 × 10^{-2} mbar) gave a colorless oil. Yield: 0.11, 95%. Physical data of **12**: ^{1}H NMR (400.25 MHz, C_6D_6, 300 K): δ 4.75 (s, 4H, PhC$\underline{H_2}$), 6.99−7.04 (m, 2H, p-PhCH$_2$), 7.06−7.12 (m, 4H, m-PhCH$_2$), 7.12−7.18 (m, 6H, m/p-PhSi), 7.24 (d, $^3J(H,H)$ = 7.6 Hz, 4H, tito-PhCH$_2$), 7.80−7.84 (m, 4H, o-PhSi). ^{13}C{^{1}H} NMR (100.65 MHz, C_6D_6, 300 K): δ 65.3 (O$\underline{C}$H$_2$Ph), 126.9 (o-PhCH$_2$), 127.4 (p-PhCH$_2$), 128.3 (m-PhSi), 128.5 (m-PhCH$_2$), 130.7 (p-PhSi), 133.0 (i-PhSi), 135.4 (o-PhSi), 140.8 (i-PhCH$_2$). MS (EI, m/z, [%]): 91 ([C$_7$H$_7$]$^+$) [100], 167 ([C$_8$H$_{11}$O$_2$Si]$^+$) [35], 227 ([C$_{13}$H$_{11}$O$_2$Si]$^+$) [33], 240 ([C$_{14}$H$_{12}$O$_2$Si]$^+$) [30], 305 ([M − C$_7$H$_7$]$^+$) [42], 318 ([M − C$_6$H$_6$]$^+$) [38], 319 ([M − Ph]$^+$) [17], 395 ([M − H]$^+$) [5]. IR (film, KBr, cm^{-1}): ν 3088 m, 3068 s, 3049 s, 3029 s, 3004 m, 2930 m, 2866 s, 1960 m, 1892 m, 1827 m, 1777 w, 1606 w, 1591 m, 1496 m, 1454 s, 1429 s, 1379 s, 1306 m, 1254 m, 1209 s, 1185 m, 1156 m, 1103 vs, 1067 vs, 1027 s, 998 m, 912 m, 854 s,796 s, 733 vs, 719 s, 697 vs, 589 m, 523 s, 492 s, 459 m.

X-ray Structure Determinations. The intensity data for compounds **2**, **3**, **8**, and **9** were collected on a Nonius Kappa-CCD diffractometer using graphite-monochromated Mo Kα radiation. Data were corrected for Lorentz and polarization

effects but not for absorption effects.[35,36] Crystyllographic data as well as structure solution and refinement details are summarized in Table 2 in the Supporting Information. The structures were solved by direct methods (SHELXS)[37] and refined by full-matrix least-squares techniques against F_o^2 (SHELXL-97).[38] For compounds **8** and **9** the hydride ions were located by difference Fourier synthesis and refined isotropically. The hydrogen atoms were included at calculated positions with fixed thermal parameters. All non-hydrogen atoms were refined anisotropically.[38] XP (SIEMENS Analytical X-ray Instruments, Inc.) was used for structure representations.

Computational Methodology. All geometry optimizations were performed with the gradient-corrected hybrid B3LYP[39] density functional using the quantum chemical program package Turbomole.[40] The TZVP basis set based on the work of Schäfer et al.[41] was employed for the first-row atoms as implemented in Turbomole. For the zinc ions a Stuttgart relativistic pseudopotential (known as ECP 10 MDF) has been employed.[42] All species found on the hypersurface were characterized as energetic minima or transition structures via vibrational analyses. Default convergence criteria were used, and no symmetry was employed in all the calculations. The relative stabilities are reported as gas phase Gibbs free energies containing standard thermochemical (298 K) and vibrational corrections. The calculation of partial charges and also the natural population analysis was performed at the same level of theory as implemented in the Gaussian program package.[43]

Acknowledgment. We thank the Deutsche Forschungsgemeinschaft (DFG, Bonn/Germany) for generous financial support. M.K. wishes to express his gratitude to the Jena Graduate Academy of the Friedrich-Schiller-Universität Jena, Germany, for a Ph.D. grant.

Supporting Information Available: CIF files giving data collection and refinement details and positional coordinates of all atom as well as the Cartesian coordinates and structures of all calculated molecules. This material is available free of charge via the Internet at http://pubs.acs.org. In addition, crystallographic data (excluding structure factors) have also been deposited with the Cambridge Crystallographic Data Centre as supplementary publication CCDC-764929 for **2**, CCDC-764930 for **3**, CCDC-764931 for **9**, and CCDC-764932 for **8**. Copies of the data can be obtained free of charge on application to CCDC, 12 Union Road, Cambridge CB2 1EZ, UK [e-mail: deposit@ccdc.cam.ac.uk].

(35) *COLLECT*, Data Collection Software; Nonius B.V.: Netherlands, 1998.
(36) Processing of X-Ray Diffraction Data Collected in Oscillation Mode: Otwinowski, Z.; Minor, W.; Carter, C. W.; Sweet, R. M., Eds.; *Macromolecular Crystallography, Part A*, Methods in Enzymology, Vol. *276*; Academic Press: New York, 1997; pp 307−326.
(37) Sheldrick, G. M. *Acta Crystallogr., Sect. A* **1990**, *46*, 467–473.
(38) Sheldrick, G. M. *SHELXL-97* (Release 97-2); University of Göttingen: Germany, 1997.
(39) (a) Becke, A. D. *J. Chem. Phys.* **1993**, *98*, 5648–5652. (b) Lee, C.; Yang, W.; Parr, R. G. *Phys. Rev. B* **1988**, *37*, 785–789.
(40) (a) Weigend, F.; Häser, M.; Patzelt, H.; Ahlrichs, R. *Chem. Phys. Lett.* **1998**, *294*, 143–152. (b) Haase, F.; Ahlrichs, R. *J. Comput. Chem.* **1993**, *14*, 907–912. (c) Ahlrichs, R.; Bär, M.; Häser, M.; Horn, H.; Kölmel, C. *Chem. Phys. Lett.* **1989**, *162*, 165–169. (d) Moller, C.; Plesset, M. S. *Phys. Rev.* **1934**, *46*, 618–622.
(41) Schäfer, A.; Huber, C.; Ahlrichs, R. *J. Chem. Phys.* **1994**, *100*, 5829–5835.
(42) Dolg, M.; Wedig, U.; Stoll, H.; Preuss, H. *J. Chem. Phys.* **1987**, *86*, 866–872.
(43) Frisch, M. J.; et al. *Gaussian 03*; Gaussian, Inc.: Wallingford, CT, 2004.